Reactions ^{50}Cr(p,γ)^{51}Mn and ^{50}Cr(p,p$'\gamma$)^{50}Cr from 2.5 to 3.1 MeV

G. U. Din
Van de Graaff Laboratory, Department of Physics, King Saud University, Riyadh, Saudi Arabia

J. A. Cameron
Tandem Accelerator Laboratory, McMaster University, Hamilton, Ontario, Canada L8S 4K1
(Received 22 February 1988)

The reactions ^{50}Cr(p,p$'\gamma$)^{50}Cr and ^{50}Cr(p,γ)^{51}Mn have been used to investigate resonances in ^{51}Mn in the range $2.5 < E_p < 3.1$ MeV ($7.7 < E_x < 8.3$ MeV). Eighty resonances, some of which are unresolved doublets, were found. Gamma-ray spectra were measured for thirty resonances which populated bound levels in ^{51}Mn up to an excitation energy of 5.174 MeV. Angular distributions were measured in the (p,p$'\gamma$) and (p,γ) channels for forty-eight resonances. These measurements and capture spectra allow spin assignments to be made for about sixty resonances. A $\frac{9}{2}^+$ core excited state has been found at $E_p = 2.798$ (8.012 MeV) and its decay measured to high spin bound levels including two previously unreported levels at 4.463 and 4.741 MeV.

I. INTRODUCTION

Over the last few years, a general gamma-ray survey of resonant states in the ^{50}Cr + p system has been made.[1–4] The proton energy range 3.08–3.36 MeV contains[1] the fragmented analogs of two $\frac{9}{2}^+$ ^{51}Cr levels. From 1.7 to 2.5 MeV the (p,γ) reaction[2] revealed a number of analog states and clarified the spins and decay modes of many bound states. In this energy region, a core excited $\frac{9}{2}^+$ resonance was found.[3] The region from 1.0 to 1.5 MeV has been reexamined for the presence of expected $l=3$ analog states.[4] Here we report a study of the region from 2.5 to 3.1 MeV. Few strong analogs are expected except for the $\frac{5}{2}^+$ states which occur in ^{51}Cr at 3.98 and 4.07

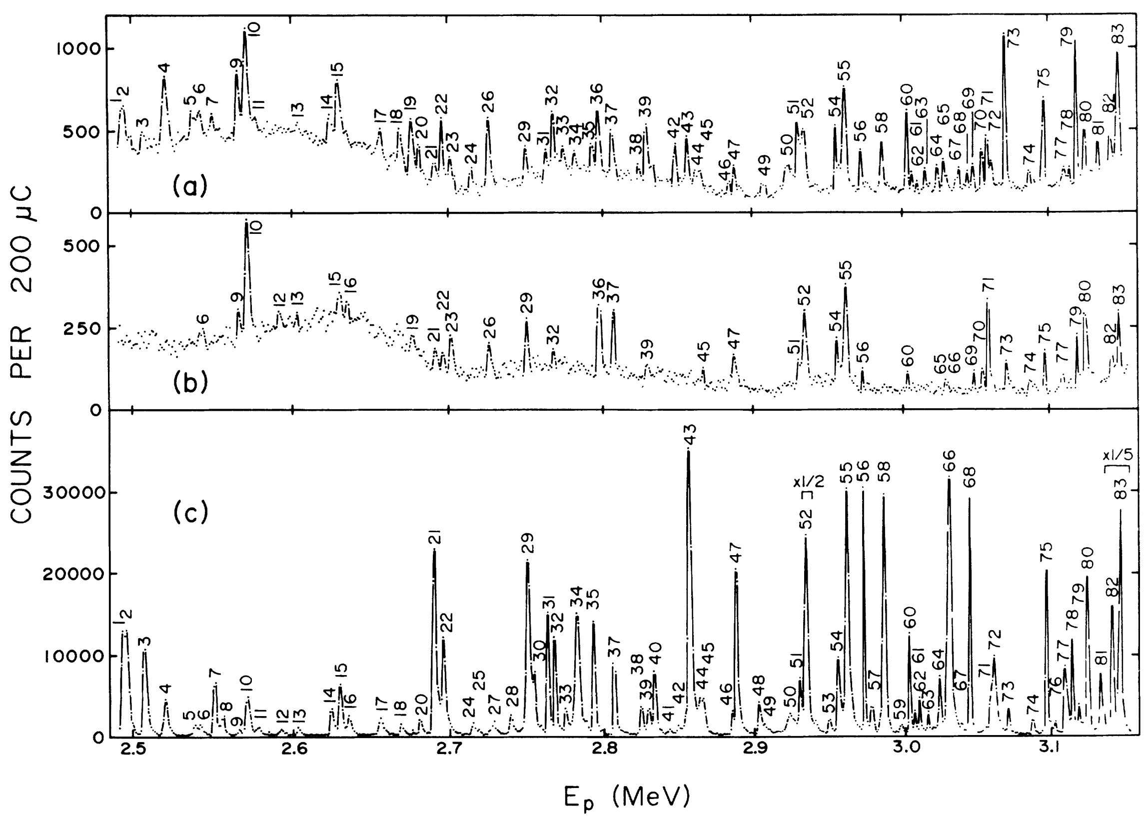

FIG. 1. Gamma-ray yield curve for ^{50}Cr + p. (a) (p,γ) with a γ window 2.7 to 5.1 MeV, (b) (p,γ) 6.2 to 8.4 MeV. (c) (p,p$'\gamma$), $E_\gamma = 0.783$ MeV.

TABLE I. Resonances in $^{50}Cr + p$ from 2.5 to 3.15 MeV.

No.	E_p (MeV)	E_x (MeV)	Spectrum	(p,p'γ)	(p,γ)	Assignment
1	2.493	7.715	$\frac{1}{2}^-, \frac{3}{2}$	$\frac{3}{2}$	$\frac{3}{2}^-$	$\frac{3}{2}^-$[a]
2	2.496	7.718	$\frac{1}{2}^-, \frac{3}{2}, \frac{5}{2}^-$			$(\frac{1}{2}^-, \frac{3}{2}, \frac{5}{2}^-)$[b]
3	2.507	7.729		$\frac{5}{2}^-$		$\frac{5}{2}^-$[b]
4*A*	2.520	7.741		$\frac{5}{2}^+$		$\frac{5}{2}^+$
4*B*	2.521	7.742	$\frac{1}{2}, \frac{3}{2}$		$\frac{1}{2}$	$\frac{1}{2}$[c]
5	2.539	7.760	$\frac{3}{2}^-, \frac{5}{2}, \frac{7}{2}^-$	$\frac{5}{2}^+$		$\frac{5}{2}^+$[d]
6	2.542	7.763				
7	2.551	7.772	$\frac{3}{2}, \frac{5}{2}, \frac{7}{2}$	$\frac{3}{2}^-$		$\frac{3}{2}^-$
8	2.556	7.777				
9	2.566	7.787	$\frac{3}{2}^-, \frac{5}{2}, \frac{7}{2}^-$	$\frac{5}{2}^-$	$\frac{5}{2}^-$	$\frac{5}{2}^-$
10	2.571	7.792	$\frac{3}{2}^-, \frac{5}{2}, \frac{7}{2}^-$	$\frac{3}{2}^-, \frac{5}{2}^-$	$\frac{5}{2}$	$\frac{5}{2}^-$
11	2.579	7.799				d
12	2.593	7.813				
13	2.603	7.823				
14	2.625	7.844	$\frac{3}{2}^-, \frac{5}{2}, \frac{7}{2}^-$	$\frac{5}{2}^+$		$\frac{5}{2}^+$
15	2.630	7.849	$\frac{1}{2}^-, \frac{3}{2}, \frac{5}{2}, \frac{7}{2}^+$	$\frac{3}{2}^-$	$\frac{3}{2}^-$	$\frac{3}{2}^-$
16	2.635	7.855	$\frac{3}{2}^-, \frac{5}{2}, \frac{7}{2}^-$	$\frac{5}{2}^-$		$\frac{5}{2}^-$
17	2.656	7.875	$\frac{1}{2}, \frac{3}{2}$	$\frac{1}{2}$		$\frac{1}{2}$
18	2.669	7.887	$\frac{3}{2}^-, \frac{5}{2}, \frac{7}{2}^-$	$\frac{5}{2}^+$	$\frac{5}{2}$	$\frac{5}{2}^+$
19	2.676	7.895	$\frac{1}{2}^-, \frac{3}{2}, \frac{5}{2}^-$			$(\frac{1}{2}^-, \frac{3}{2}, \frac{5}{2}^-)$
20	2.681	7.899	$\frac{1}{2}^-, \frac{3}{2}, \frac{5}{2}^-$	$\frac{5}{2}$	$\frac{1}{2}, \frac{3}{2}^-$	$\frac{1}{2}, \frac{3}{2}^-, \frac{5}{2}$
21	2.690	7.908		$\frac{3}{2}^-, \frac{5}{2}^-$		$\frac{5}{2}^-$[b]
22	2.696	7.914	$\frac{3}{2}^-, \frac{5}{2}^-$	$\frac{3}{2}^-$		$\frac{3}{2}^-$
23	2.701	7.919	$\frac{3}{2}^-, \frac{5}{2}, \frac{7}{2}^-$			$(\frac{3}{2}^-, \frac{5}{2}, \frac{7}{2}^-)$
24	2.715	7.933	$\frac{1}{2}^-, \frac{3}{2}, \frac{5}{2}, \frac{7}{2}^-$		$\frac{3}{2}^-, \frac{5}{2}^-, \frac{7}{2}$	$\frac{3}{2}^-, \frac{5}{2}^-, \frac{7}{2}^{(-)}$
25	2.719	7.936	$\frac{1}{2}^-, \frac{3}{2}, \frac{5}{2}^+$			$(\frac{1}{2}^-, \frac{3}{2}, \frac{5}{2}^+)$
26	2.726	7.944	$\frac{1}{2}^-, \frac{3}{2}, \frac{5}{2}, \frac{7}{2}^-$		$\frac{3}{2}^-$	$\frac{3}{2}^-$[c,d]
27	2.728	7.946		$\frac{5}{2}^+$		$\frac{5}{2}^+$
28	2.740	7.957		$\frac{5}{2}^+$		$\frac{5}{2}^+$
29	2.751	7.967	$\frac{1}{2}^-, \frac{3}{2}, \frac{5}{2}, \frac{7}{2}^-$	$\frac{3}{2}^-$		$\frac{3}{2}^-$
30	2.755	7.971		$\frac{1}{2}, \frac{3}{2}^-$		$\frac{1}{2}, \frac{3}{2}^-$
31	2.765	7.981		$\frac{5}{2}^-$		$\frac{5}{2}^-$
32	2.768	7.985	$\frac{3}{2}^-, \frac{5}{2}, \frac{7}{2}^-$	$\frac{5}{2}^+$		$\frac{5}{2}^+$
33	2.775	7.991		$\frac{3}{2}^-$		$\frac{3}{2}^-$
34	2.783	7.999		$\frac{1}{2}$		$\frac{1}{2}$
35	2.794	8.010		$\frac{3}{2}^-$		$\frac{3}{2}^-$
36	2.798	8.013	$\frac{7}{2}^-, \frac{9}{2}, \frac{11}{2}^-$		$\frac{9}{2}$	$\frac{9}{2}^+$
37	2.807	8.023	$\frac{3}{2}^-, \frac{5}{2}, \frac{7}{2}^-$	$\frac{5}{2}^+$		$\frac{5}{2}^+$
38	2.826	8.041		$\frac{1}{2}$		$\frac{1}{2}$
39	2.830	8.045	$\frac{1}{2}^-, \frac{3}{2}, \frac{5}{2}^+$	$\frac{1}{2}, \frac{3}{2}$	$\frac{3}{2}^-$	$\frac{3}{2}^-$[d]
40	2.835	8.050		$\frac{5}{2}^+$		$\frac{5}{2}^+$
41	2.843	8.058				
42	2.849	8.064	$\frac{1}{2}^-, \frac{3}{2}, \frac{5}{2}^-$	$\frac{3}{2}^-$	$\frac{3}{2}$	$\frac{3}{2}^-$
43	2.857	8.072	$\frac{3}{2}^-, \frac{5}{2}, \frac{7}{2}^-$	$\frac{3}{2}^-$	$\frac{3}{2}^-, \frac{5}{2}$	$\frac{3}{2}^-$[f]

TABLE I. (*Continued*).

No.	E_p (MeV)	E_x (MeV)	Spectrum	(p,p′γ)	(p,γ)	Assignment
44	2.863	8.078				
45	2.866	8.080				b
46	2.885	8.099				
47	2.887	8.102	$\frac{1}{2}^-, \frac{3}{2}, \frac{5}{2}, \frac{7}{2}^-$	$\frac{5}{2}^+$		$\frac{5}{2}^+$
48	2.903	8.117		$\frac{5}{2}^+$		$\frac{5}{2}^+$
49	2.908	8.122				
50	2.924	8.138				
51	2.930	8.143	$\frac{5}{2}^-, \frac{7}{2}^-$	$\frac{3}{2}^-$	$\frac{7}{2}^-$	$\frac{7}{2}^-$ [b]
52	2.934	8.147	$\frac{1}{2}^-, \frac{3}{2}, \frac{5}{2}, \frac{7}{2}^-$	$\frac{1}{2}$	$\frac{3}{2}^-, \frac{5}{2}^-, \frac{7}{2}$	$\frac{3}{2}^-, \frac{5}{2}^-, \frac{7}{2}^{(-)}$
53	2.950	8.163				
54	2.956	8.169	$\frac{1}{2}^-, \frac{3}{2}, \frac{5}{2}, \frac{7}{2}^-$	$\frac{3}{2}$	$\frac{3}{2}^-, \frac{5}{2}$	$\frac{3}{2}$
55	2.962	8.174	$\frac{1}{2}^-, \frac{3}{2}, \frac{5}{2}, \frac{7}{2}^-$	$\frac{1}{2}, \frac{3}{2}^-$	$\frac{3}{2}, \frac{5}{2}^-,$	$\frac{3}{2}^-$ [e]
56	2.974	8.187	$\frac{3}{2}^-, \frac{5}{2}, \frac{7}{2}^-$	$\frac{5}{2}^+$		$\frac{5}{2}^+$
57	2.978	8.190				
58	2.987	8.199	$\frac{3}{2}^-$	$\frac{3}{2}^-$		$\frac{3}{2}^-$
59	2.998	8.210				
60	3.004	8.216	$\frac{1}{2}^-, \frac{3}{2}^-, \frac{5}{2}^-$	$\frac{5}{2}$&	$\frac{3}{2}^-$&$\frac{5}{2}^-$	$\frac{3}{2}^-$&$\frac{5}{2}^-$
61	3.007	8.219	$\frac{5}{2}, \frac{7}{2}, \frac{9}{2}$			$(\frac{5}{2}, \frac{7}{2}, \frac{9}{2})$
62	3.011	8.223		$\frac{5}{2}^+$&$\frac{1}{2}$		$\frac{5}{2}^+$&$\frac{1}{2}$
63	3.016	8.228				
64	3.024	8.236		$\frac{1}{2}$		$\frac{1}{2}$
65	3.029	8.241				
66	3.031	8.243		$\frac{3}{2}^-$		$\frac{3}{2}^-$
67	3.039	8.250				d
68	3.045	8.256	$\frac{1}{2}^-, \frac{3}{2}, \frac{5}{2}^-$	$\frac{3}{2}^+, \frac{5}{2}^-$		$\frac{3}{2}^+, \frac{5}{2}^-$ [b]
69	3.049	8.260	$\frac{3}{2}^-, \frac{5}{2}, \frac{7}{2}, \frac{9}{2}^-$	$\frac{3}{2}^-$	$\frac{5}{2}, \frac{7}{2}^-, \frac{9}{2}$	$\frac{5}{2}^-, \frac{7}{2}^-$
70	3.055	8.266	$\frac{3}{2}^-, \frac{5}{2}, \frac{7}{2}, \frac{9}{2}^-$			$(\frac{3}{2}^-, \frac{5}{2}, \frac{7}{2})$
71	3.058	8.269	$\frac{3}{2}^-, \frac{5}{2}, \frac{7}{2}^-$		$\frac{5}{2}^-$	$\frac{5}{2}^-$
72	3.061	8.272	$\frac{1}{2}^-, \frac{3}{2}, \frac{5}{2}^-$	$\frac{3}{2}^-$		$\frac{3}{2}^-$
73	3.071	8.281	$\frac{1}{2}^-, \frac{3}{2}, \frac{5}{2}^+$	$\frac{3}{2}^-$	$\frac{3}{2}^-, \frac{5}{2}$	$\frac{3}{2}^-$ [g]
74	3.087	8.298				
75	3.097	8.307	$\frac{1}{2}^-, \frac{3}{2}, \frac{5}{2}^+$	$\frac{5}{2}^+$&$\frac{1}{2}$		$\frac{1}{2}^-$&$\frac{5}{2}^+$ [d,h]
76	3.103	8.313		$\frac{3}{2}^-$		$\frac{3}{2}^-$ [h]
77	3.110	8.320				c
78	3.115	8.325				$\frac{3}{2}^-$ [h]
79	3.120	8.329				$\frac{1}{2}$ [h]
80	3.126	8.335				$\frac{5}{2}^+$ [h]
81	3.135	8.344				$\frac{3}{2}^-$&$\frac{9}{2}^+$ [h]
82	3.143	8.352				$\frac{5}{2}^+$ [h]
83	3.149	8.358				$\frac{5}{2}^+$ [h]

[a]Reference 3.
[b]Reference 6: $\frac{5}{2}^+$.
[c]References 6 and 7: $\frac{1}{2}^-$.
[d]Reference 6: $\frac{1}{2}^+$.
[e]References 6 and 7: $\frac{3}{2}^-$.
[f]References 6 and 7: $\frac{1}{2}^-$&$\frac{3}{2}^-$.
[g]References 6 and 7: $\frac{1}{2}^+$&$\frac{3}{2}^-$.
[h]Reference 1.

MeV, $\frac{1}{2}^-$ and $\frac{3}{2}^-$ levels at 4.04 and 3.77 MeV, respectively, and a $\frac{5}{2}^-$ level at 3.35 MeV.[5] The region above $E_p=2$ MeV is accessible to elastic scattering studies. The TUNL group has reported (p,p) and (p,p′) surveys covering the range 1.8–3.3 MeV (Refs. 6 and 7) and suggested analog candidates in the above cases. Although there have been a number of (^{3}He,d) measurements,[5] results are unavailable for the region above 6.5 MeV.

II. EXPERIMENT

The study was carried out using the McMaster KN 3MV Van de Graaff and FN tandem accelerators. Equipment and methodology were as described in the earlier reports.[1–4] The yield curve, using a 10 μg/cm^2 ^{50}Cr target was measured in 2 kHz (1.1 keV) steps from 2.49 to 3.15 MeV with observation in the (p,p′γ) channel and with

TABLE II. Primary capture decays in ^{50}Cr + p.

E_f (MeV) \ Res. No.	1	2	4	9	10	14	15	18	19	22
0	13		2	22	44	11	28	56	21	12
0.238			1	32	21	6				8
1.140										
1.488										
1.817										
1.825			23	30		20	15	7	45	
1.959	60		21						9	17
2.140			21		6		6			25
2.256					6		9			16
2.276										
2.310			3			11	3			
2.416					15					
2.702		100	6			22				
2.841	11									
2.893										
2.914			4						5	
2.985				16	6		12			
3.029										
3.049										
3.131					2	30			5	
3.281										
3.292							6		3	
3.423									9	8
3.554			3				5			
3.694			5					8		5
3.730										
3.825										
3.835										
3.893			2				2			
3.939										
4.000										
4.013										
4.153	4		6							
4.200	8									
4.205							4			
4.352							4			
4.362										
4.463										
4.488	4									
4.523								4		
4.601								4		
4.739										
4.883								13	3	
4.927										4
5.064							6	4		
5.074										
5.129								4		5
5.174			3							

two wide (p,γ) windows, with the result shown in Fig. 1. Altogether 83 resonances were clearly identified. These are listed in Table I. Resonances 1 and 2, which form a close doublet, correspond to no. 72 of Ref. 2, while at the high energy end resonances 75 to 83 correspond to nos. 1 to 7 of Ref. 1. The agreement in energy with the earlier work, and with the results of the higher resolution (p,p) work,[6] is excellent.

At the strong (p,γ) peaks, spectra were measured. The branching ratios derived using the measured relative efficiency of the dètector are contained in Table II. The example shown in Fig. 2, for resonance 36, illustrates the quality of the data obtained. The good resolution, about 7 keV FWHM at 8 MeV, made weak transitions, such as

TABLE II. (*Continued*).

Res. No. / E_f (MeV)	24	26	29	36	37	39	42	47	51	52
0	21	15	71		46	25	5	61	19	56
0.238				50	28			4		
1.140				6					30	
1.488				27						
1.817	36									
1.825		68	29			20	17			7
1.959							20			
2.140		6				23	10	2		
2.256		3					6	4		
2.276						32				
2.310	11						2		10	
2.416										
2.702	21				26		2	13		
2.841									12	
2.893				2				8		
2.914										
2.985		2								
3.029										
3.049										
3.131		3						8	9	
3.281	11								11	
3.292									9	
3.423							3			
3.554							6			
3.694										8
3.730				2						
3.825										
3.835				4						
3.893										
3.939										
4.000				3						
4.013										
4.153										
4.200										
4.205		3					2			
4.352							2			
4.362							3			
4.463				3						
4.488										
4.523										4
4.601										4
4.739				3						
4.883										13
4.927							4			
5.064										
5.074							3			4
5.129							15			
5.174										4

that at 6.881 MeV, observable. Most of the impurity lines, from room radioactivity—^{40}K, ^{60}Co, and U series isotopes—occur at low energy, as do lines from target impurities such as Al, Na, and Si. The only prominent high energy impurity is from ^{19}F(p,$\alpha\gamma$) ^{16}O at 6.130 MeV.

Angular distributions of the (p,p$'\gamma$) $2^+ \rightarrow 0^+$ transition and, where feasible, capture transitions were measured and fitted to obtain spin-parity assignments, given in detail in Table III and summarized in Table I.

Generally, in cases where angular distributions were measured for two or three major capture branches,

TABLE II. (*Continued*).

E_f (MeV) \ Res. No.	54	55	56	58	60	68	69	70	71	75
0	40	46	19		7	7			48	20
0.238	42		10	2	7		57	46	16	
1.410										
1.488										
1.817		20	20	7					12	11
1.825										
1.959				19	17	8				11
2.140		5	7		31				6	5
2.256									1	
2.276				7						
2.310	9		26			76				7
2.416	9		3						3	
2.702			10							
2.841			3	8	10		7			12
2.893										
2.914				4	9				2	
2.985				23						
3.029								8		
3.049								6	5	
3.131					3	9				10
3.281							10	19		
3.292		4								
3.423									2	
3.554					3				2	5
3.694		4		11						
3.730										
3.825		4					20			
3.835									1	
3.893		2			3					
3.939									1	
4.000										
4.013								21	1	
4.153			2		3					3
4.200										
4.205										
4.352										
4.362		4								4
4.463										
4.488										
4.523					4		6			
4.601										
4.739										
4.883		9								
4.927				5						
5.064										
5.074										
5.129					3					7
5.174		2		14						5

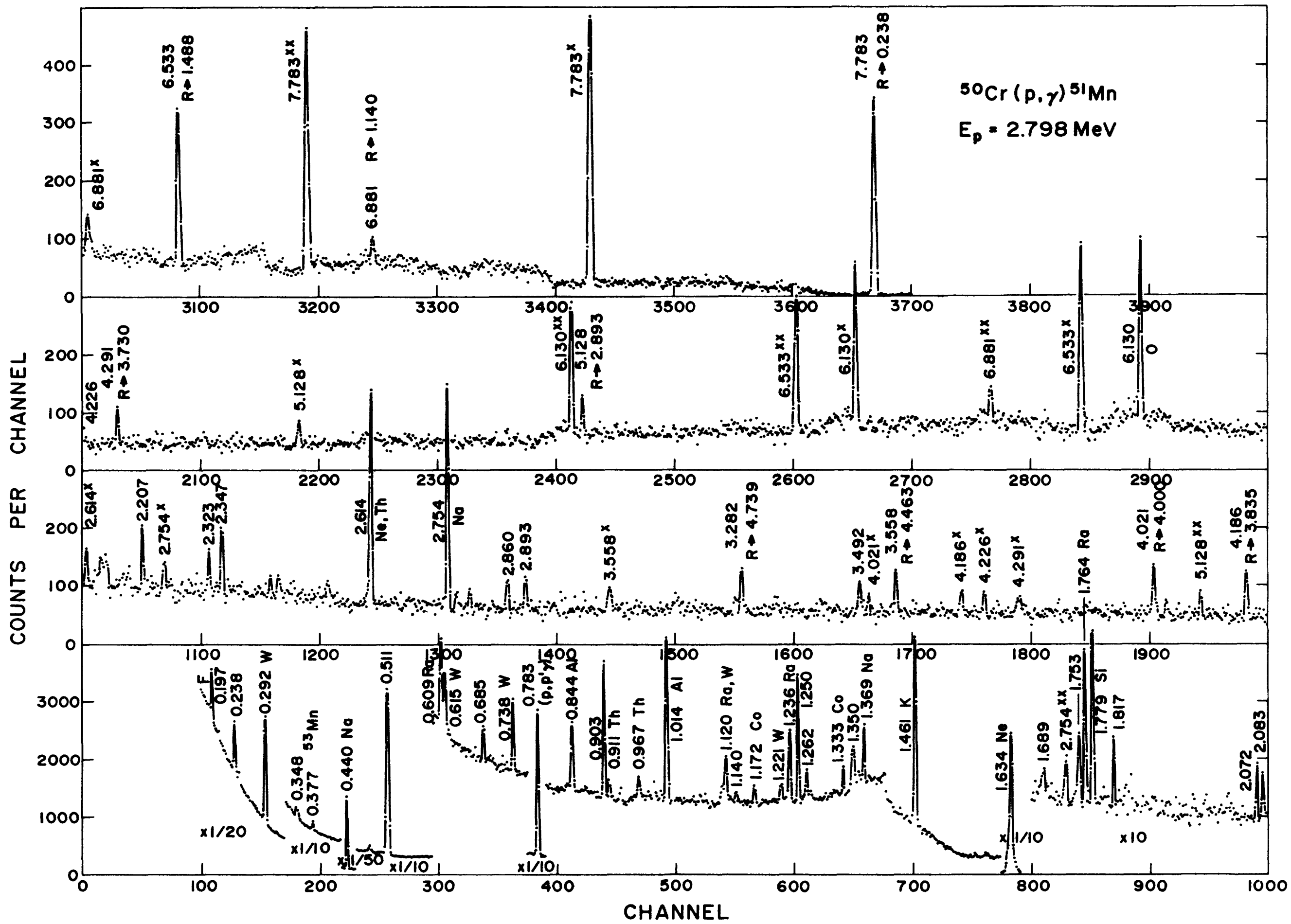

FIG. 2. Spectrum observed at resonance no. 36. The primary decay branches are identified, along with the strongest background lines from target impurities and room radioactivity.

unambiguous assignments are possible. The (p,p$'\gamma$) angular distributions, even on spin-zero targets, are somewhat ambiguous of interpretation and some restriction of exit channel angular momenta must be made.[1,8] In cases where the spin choice is dependent on spectra only, assuming only $M1$, $E1$, and $E2$ transitions to have significant strength, the tentative assignments made are indicated in parentheses. In Table I, assignments connected by an ampersand indicate unresolved doublets, suggested by incompatible spin assignments. Wherever possible, these were confirmed by measuring spectra at 1 kHz intervals. The footnotes to Table I indicate the regions of overlap with Refs. 1 and 3, and the few cases of disagreement with Refs. 6 and 7.

III. DISCUSSION

A. Bound states of ^{51}Mn

Although the decays of many resonances were observed, only two new bound states beyond those already known[2,5] were found. These will be mentioned in Sec. III B below. Almost all the levels with $J \le \frac{11}{2}$ up to about 4 MeV in ^{51}Mn and surveyed in Ref. 5 were excited in this work.

B. Core excited $\frac{9}{2}^+$ resonances

The same properties that distinguish the $g_{9/2}$ IAS and make its fragments noticeable[1] have allowed us to identify $T=\frac{1}{2}$ $\frac{9}{2}^+$ "orphan" states in ^{51}Mn, ^{53}Mn,[3] and in ^{59}Cu.[11] However, unlike the situation encountered in ^{59}Cu of strong γ decay to an antianalog state, or that of the analogs in ^{51,53}Mn, which proton decay to the target 4^+ state, the orphans in ^{51}Mn decay primarily to the high-spin members of the $f_{7/2}^{-3}$ multiplet, with $J^\pi=\frac{7}{2}^-$, $\frac{9}{2}^-$, $\frac{11}{2}^-$. The decay branching of resonance no. 36, obtained from the spectrum shown in Fig. 2, indicates this preference and the angular distributions clearly select spin $\frac{9}{2}$. Since an $l=5, \frac{9}{2}^-$ resonance at this energy is unlikely, we assign $J^\pi=\frac{9}{2}^+$. In addition to the three main transitions, weaker decays to levels above 1.488 MeV were found, as indicated in Fig. 3. The levels at 4.463 and 4.739 MeV have not previously been observed. The

TABLE III. Angular distribution results.

Res. No.	E_f	J_f^π	A_2	A_4	J_i^π
1	inelastic		0.45(2)	0.06(2)	$\frac{3}{2}$
	0	$\frac{5}{2}^-$	−0.51(8)	0.05(9)	$\frac{3}{2}^-,\frac{7}{2}$
	1.817	$\frac{3}{2}^-$	0.76(19)	−0.28(20)	$\frac{3}{2}^-,\frac{5}{2}$
	2.702	$\frac{3}{2}^-$	−0.37(9)	0.14(11)	$\frac{3}{2}^-,\frac{5}{2}$
3	inelastic		0.43(2)	−0.09(2)	$\frac{5}{2}^-$
4	inelastic		0.30(2)	−0.35(2)	$\frac{5}{2}^+$&
	1.817	$\frac{3}{2}^-$	0.06(6)	−0.10(7)	$\frac{1}{2},\frac{3}{2},\frac{5}{2}^-$
	1.959	$\frac{1}{2}^-$	−0.05(7)	0.07(7)	$\frac{1}{2},\frac{3}{2}^-$
	2.140	$\frac{3}{2}^-$	−0.19(12)	0.04(14)	$\frac{1}{2},\frac{3}{2}^-,\frac{5}{2}$
5	inelastic		0.46(2)	−0.54(2)	$\frac{5}{2}^+$
7	inelastic		0.24(2)	−0.02(2)	$\frac{3}{2}^-$
9	inelastic		0.44(2)	−0.24(2)	$\frac{5}{2}^-$
	0	$\frac{5}{2}^-$	0.22(18)	−0.46(11)	$\frac{5}{2}^-,\frac{7}{2}^-$
	0.238	$\frac{7}{2}^-$	−0.21(18)	−0.18(8)	$\frac{5}{2}^-,\frac{7}{2}^-$
	1.825	$\frac{3}{2}^-$	0.79(21)	−0.57(15)	$\frac{5}{2}^-$
10	inelastic		0.37(2)	−0.07(2)	$\frac{3}{2}^-,\frac{5}{2}^-$
	0	$\frac{5}{2}^-$	0.52(2)	0.02(2)	$\frac{5}{2}$
	0.238	$\frac{7}{2}^-$	−0.17(3)	−0.03(2)	$\frac{5}{2},\frac{7}{2}^-,\frac{9}{2}$
	2.140	$\frac{3}{2}^-$	−0.44(4)	0.10(5)	$\frac{3}{2}^-,\frac{5}{2}$
	2.416	$\frac{7}{2}^-$	−0.01(5)	−0.06(6)	$\frac{3}{2}^-,\frac{5}{2},\frac{7}{2}^-,\frac{9}{2}^-$
14	inelastic		0.52(2)	−0.54(2)	$\frac{5}{2}^+$
15	inelastic		0.30(2)	0.00(2)	$\frac{3}{2}^-$
	0	$\frac{5}{2}^-$	−0.50(3)	0.08(4)	$\frac{3}{2}^-,\frac{7}{2}$
	1.825	$\frac{3}{2}^-$	0.22(5)	−0.25(6)	$\frac{3}{2}^-,\frac{5}{2}$
16	inelastic		0.24(2)	0.11(2)	$\frac{5}{2}^-$
17	inelastic		−0.05(2)	−0.01(2)	$\frac{1}{2}$
18	inelastic		0.52(2)	−0.54(2)	$\frac{5}{2}^+$
	0.238	$\frac{7}{2}^-$	−0.22(9)	−0.15(11)	$\frac{5}{2},\frac{7}{2}^-,\frac{9}{2}$
	1.817	$\frac{3}{2}^-$	−0.64(6)	−0.05(7)	$\frac{3}{2}^-,\frac{5}{2}$
20	inelastic		0.19(2)	−0.29(2)	$\frac{5}{2}$
	1.825	$\frac{3}{2}^-$	−0.14(10)	−0.22(12)	$\frac{1}{2},\frac{3}{2}^-,\frac{5}{2}^-$
	1.959	$\frac{1}{2}^-$	−0.08(11)	−0.26(12)	$\frac{1}{2},\frac{3}{2}^-$
	2.914	$\frac{3}{2}^-$	−0.16(10)	−0.12(11)	$\frac{1}{2},\frac{3}{2}^-,\frac{5}{2}$
21	inelastic		0.33(2)	−0.06(2)	$\frac{3}{2}^-,\frac{5}{2}^-$
22	inelastic		0.06(2)	0.00(2)	$\frac{3}{2}^-$
24	0	$\frac{5}{2}^-$	−0.24(6)	−0.20(7)	$\frac{3}{2}^-,\frac{5}{2}^-,\frac{7}{2}$
	2.702	$\frac{3}{2}^-$	0.59(12)	−0.42(12)	$\frac{3}{2},\frac{5}{2}^-$
26	0	$\frac{5}{2}^-$	0.23(3)	0.03(3)	$\frac{3}{2}^-,\frac{5}{2}^-,\frac{7}{2}^-$
	2.140	$\frac{3}{2}^-$	0.80(6)	0.02(6)	$\frac{3}{2}^-,\frac{7}{2}^-$
	2.841	$\frac{1}{2}^-$	−0.51(6)	0.18(9)	$\frac{3}{2}$
27	inelastic		0.28(4)	−0.39(4)	$\frac{5}{2}^+$&$\frac{3}{2}$ (R26)
28	inelastic		0.43(2)	−0.46(2)	$\frac{5}{2}^+$&$\frac{1}{2}$
29	inelastic		0.13(2)	−0.05(2)	$\frac{3}{2}^-$
30	inelastic		−0.06(2)	−0.02(2)	$\frac{1}{2}$
31	inelastic		0.40(2)	−0.07(2)	$\frac{5}{2}^-$

TABLE III. (*Continued*).

Res. No.	E_f	J_f^π	A_2	A_4	J_i^π
32	inelastic		0.52(2)	−0.50(2)	$\frac{5}{2}^+$
33	inelastic		0.27(2)	0.02(2)	$\frac{3}{2}^-$
34	inelastic		0.03(2)	0.02(2)	$\frac{1}{2}$
35	inelastic		0.19(2)	−0.01(2)	$\frac{3}{2}^-$
36	0.238	$\frac{7}{2}^-$	−0.20(2)	0.01(2)	$\frac{5}{2},\frac{9}{2}$
	1.140	$\frac{9}{2}^-$	0.20(11)	0.33(13)	$\frac{5}{2},\frac{7}{2}^-,\frac{9}{2}$
	1.488	$\frac{11}{2}^-$	−0.35(3)	0.05(3)	$\frac{9}{2}$
37	inelastic		0.53(2)	−0.55(2)	$\frac{5}{2}^+$
38			−0.07(2)	−0.08(2)	$\frac{1}{2}$
39	inelastic		0.02(2)	0.01(2)	$\frac{1}{2},\frac{3}{2}$
	0	$\frac{5}{2}^-$	−0.11(4)	0.15(5)	$\frac{3}{2},\frac{5}{2}^-,\frac{7}{2}$
	1.825	$\frac{3}{2}^-$	−0.19(4)	−0.00(5)	$\frac{3}{2}^-,\frac{5}{2}$
	2.140	$\frac{3}{2}^-$	0.28(7)	−0.02(7)	$\frac{3}{2},\frac{5}{2}^-$
	2.276	$\frac{1}{2}^+$	−0.13(4)	−0.05(4)	$\frac{3}{2}$
40	inelastic		0.54(2)	−0.50(2)	$\frac{5}{2}^+$
42	inelastic		0.27(2)	−0.03(2)	$\frac{3}{2}^-$
	1.959	$\frac{1}{2}^-$	−0.58(6)	0.07(7)	$\frac{3}{2}$
43	inelastic		0.09(2)	−0.08(2)	$\frac{3}{2}^-$
	1.817	$\frac{3}{2}^-$	−0.56(6)	−0.08(7)	$\frac{3}{2}^-,\frac{5}{2}$
47	inelastic		0.48(2)	−0.48(2)	$\frac{5}{2}^+$
48	inelastic		0.45(2)	−0.54(2)	$\frac{5}{2}^+$
51	inelastic		0.14(2)	−0.02(2)	$\frac{3}{2}^-$
	0	$\frac{5}{2}^-$	0.12(10)	0.31(12)	$\frac{3}{2}^-,\frac{5}{2},\frac{7}{2}^-$
	0.238	$\frac{7}{2}^-$	0.20(5)	0.09(5)	$\frac{5}{2}^-,\frac{7}{2}^-,\frac{9}{2}^-$
	1.140	$\frac{9}{2}^-$	0.31(5)	−0.01(6)	$\frac{7}{2}^-,\frac{9}{2}^-$
52	inelastic		0.03(2)	−0.01(2)	$\frac{1}{2}$
	0	$\frac{5}{2}^-$	−0.36(2)	0.05(2)	$\frac{3}{2}^-,\frac{5}{2}^-,\frac{7}{2}$
54	inelastic		0.21(2)	−0.01(2)	$\frac{3}{2}^-$
	0	$\frac{5}{2}^-$	0.23(3)	0.17(4)	$\frac{3}{2}^-,\frac{5}{2},\frac{7}{2}^-$
	1.817	$\frac{3}{2}^-$	−0.29(3)	0.02(3)	$\frac{3}{2}^-,\frac{5}{2}$
55	inelastic		0.04(2)	0.00(2)	$\frac{1}{2},\frac{3}{2}^-$
	0	$\frac{5}{2}^-$	−0.13(2)	0.05(2)	$\frac{3}{2},\frac{5}{2}^-$
56	inelastic		0.52(2)	−0.59(2)	$\frac{5}{2}^+$
58	inelastic		0.21(2)	−0.04(2)	$\frac{3}{2}^-$
60	inelastic		0.25(2)	−0.25(2)	$\frac{5}{2}$&
	0	$\frac{5}{2}^-$	−0.11(12)	−0.23(15)	$\frac{1}{2},\frac{3}{2},\frac{5}{2}^-$
	0.238	$\frac{7}{2}^-$	0.30(13)	−0.54(14)	$\frac{5}{2}^-,\frac{9}{2}$
	1.959	$\frac{1}{2}^-$	−0.62(7)	0.06(8)	$\frac{3}{2}$
	2.140	$\frac{3}{2}^-$	0.15(4)	−0.04(5)	$\frac{3}{2}^-,\frac{5}{2}^-$
62	inelastic		0.45(2)	−0.44(2)	$\frac{5}{2}^+$&
64	inelastic		0.05(2)	0.04(2)	$\frac{1}{2}$
66	inelastic		0.13(2)	0.01(2)	$\frac{3}{2}^-$
68	inelastic		0.47(2)	−0.05(2)	$\frac{3}{2}^+,\frac{5}{2}^-$
69	inelastic		0.23(2)	0.01(2)	$\frac{3}{2}^-$
	0.238	$\frac{7}{2}^-$	−0.38(5)	−0.08(6)	$\frac{5}{2}^-,\frac{7}{2}^-,\frac{9}{2}$

TABLE III. (*Continued*).

Res. No.	E_f	J_f^π	A_2	A_4	J_i^π
71	0	$\frac{5}{2}^-$	0.41(2)	−0.06(2)	$\frac{3}{2}^-,\frac{5}{2}$
	0.238	$\frac{7}{2}^-$	−0.12(4)	0.01(4)	$\frac{5}{2},\frac{7}{2}^-,\frac{9}{2}^-$
	1.817	$\frac{3}{2}^-$	−0.83(4)	−0.09(5)	$\frac{5}{2}^-$
72	inelastic		0.14(2)	0.00(2)	$\frac{3}{2}^{-\,a}$
73	inelastic		0.05(2)	0.01(2)	$\frac{3}{2}^-$
	0	$\frac{5}{2}^-$	0.08(6)	0.27(7)	$\frac{3}{2}^-,\frac{5}{2},\frac{7}{2}^-$
	1.820	$\frac{3}{2}^-$	−0.22(3)	0.03(3)	$\frac{3}{2}^-,\frac{5}{2}$

[a]Not fully resolved from resonance no. 7.

cascade transitions from these and from the 3.835 and 4.000 MeV levels to high spin states suggest that their spins too are large ($J > \frac{7}{2}$). Figure 3 also includes decays of the two fragmented $g_{9/2}$ analogs and the previously reported orphan state at 7.621 MeV.

C. Analog states

Among the many resonances studied here, several may be identified as isobaric analogs of ^{51}Cr states. These are listed in Table IV where the Coulomb energy shift,

$$\Delta E_c = E_x(\mathrm{Mn}) - E_x(\mathrm{Cr}) + Q(\mathrm{Mn}\rightarrow\mathrm{Cr}) + Q(\mathrm{n}\rightarrow\mathrm{H}) ,$$

is given for each state pair. Figure 4 combines the present results with those of the earlier measurements[1,2,4] to give an overall picture of the variation of ΔE_c with excitation energy and spin.

The trends which may be seen in Fig. 4 are twofold. There seems to be little J or l dependence of the Coulomb energy, which falls after an initial rise with increasing excitation energy. The tendency to decreasing ΔE_c with increasing ΔE_x has appeared in other studies.[11,12] The review of Nolen and Schiffer,[13] aimed primarily at the systematic A,Z,T dependence of ΔE_c, does not address the question of E_x or J dependence explicitly. It does, however, provide insights useful in this connection. Single-particle wave functions in infinite wells show no E_x or J dependence of the Coulomb energy. However, multipar-

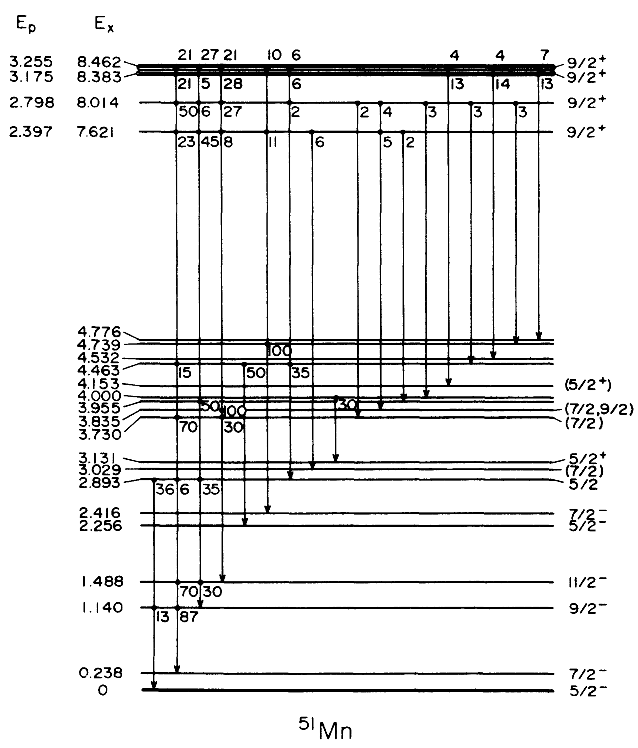

FIG. 3. Decay schemes of the $\frac{9}{2}^+$ resonances. The IAS decays, given in detail in Ref. 1, are averaged over the fragments. That for the 7.621 MeV level is from Ref. 2.

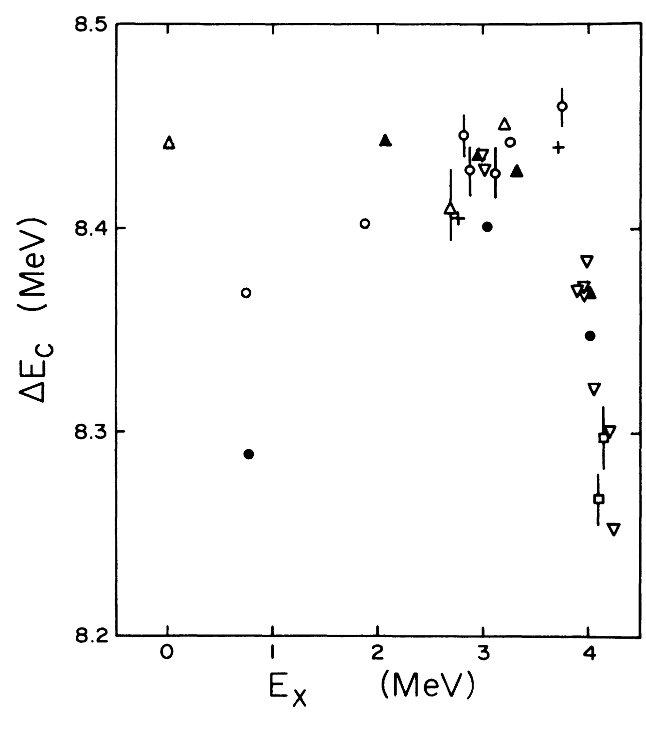

FIG. 4. Dependence of the Coulomb energy shift on excitation energy and J^π (+, $\frac{1}{2}^+$; ●, $\frac{1}{2}^-$, ○, $\frac{3}{2}^-$; ▼, $\frac{3}{2}^+$, ▽, $\frac{5}{2}^+$; ▲, $\frac{5}{2}^-$, △, $\frac{7}{2}^-$; □, $\frac{9}{2}^+$). The vertical bars suggest the width of fragmented states.

TABLE IV. Proposed isobaric analog states.

^{51}Cr [a]			^{51}Mn		
E_x (MeV)	J^π	No.	E_x (MeV)	J^π	ΔE_c (MeV)
3.263	$\frac{3}{2}^-,\frac{5}{2},\frac{7}{2}^-$	1	7.715	$\frac{3}{2}^-$	8.442
		2	7.718	$(\frac{1}{2}^-,\frac{3}{2},\frac{5}{2}^-)$	8.445
3.351	$\frac{5}{2}^-$	9	7.787	$\frac{5}{2}^-$	8.426
		10	7.792	$\frac{5}{2}^-$	8.431[b,c]
3.716	$\frac{1}{2}^+$		8.167	$\frac{1}{2}^+$	8.441[b]
3.765	$\frac{1}{2}^-,\frac{3}{2}^-$	58	8.199	$(\frac{3}{2}^-)$	8.424
3.767	$\frac{1}{2}^-,\frac{3}{2}^-$	60	8.216	$(\frac{3}{2}^-)$	8.439
3.900	$\frac{3}{2}^-,\frac{5}{2},\frac{7}{2}^-$	73	8.281	$\frac{5}{2}^+$	8.371
3.927	$\frac{3}{2}^-,\frac{5}{2}$	75	8.307	$\frac{5}{2}^+$	8.370
3.953	$\frac{3}{2}^-,\frac{5}{2},\frac{7}{2}^-$	80	8.335	$\frac{5}{2}^+$	8.372
3.977	$\frac{5}{2}^+$	82	8.352	$\frac{5}{2}^+$	8.365
		83	8.358	$\frac{5}{2}^+$	8.371[b,c,f]
3.985	$\frac{3}{2}^-,\frac{5}{2},\frac{7}{2}$		8.379	$\frac{5}{2}^+$	8.384[d]
3.990	$\frac{3}{2}^+,\frac{5}{2}^+$		8.384	$\frac{3}{2}^+$	8.384[d]
4.005	$\frac{5}{2}^-,\frac{7}{2}^-$		8.386	$\frac{5}{2}^-$	8.371[d]
4.040	$\frac{1}{2}^-$		8.398	$\frac{1}{2}$	8.348[b,d,e]
4.071	$\frac{3}{2}^+,\frac{5}{2}^+$		8.403	$\frac{5}{2}^+$	8.322[d,e,f]
4.101	$\frac{7}{2}^+,\frac{9}{2}^+$		8.384	$\frac{9}{2}^+$ (centroid)	8.273[d]
4.155	$\frac{7}{2}^+,\frac{9}{2}^+$		8.459	$\frac{9}{2}^+$ (centroid)	8.294[d]
4.189	$\frac{3}{2}^+,\frac{5}{2}^+$		8.499	$\frac{5}{2}^+$	8.300[d,e,f]
4.258	$\frac{3}{2}^+,\frac{5}{2}^+$		8.521	$\frac{5}{2}^+$	8.253[d,e,f]

[a]Reference 4.
[b]Suggested in Ref. 5.
[c]Suggested in Ref. 8.
[d]Reference 1.
[e]Suggested in Ref. 9.
[f]Suggested in Ref. 10.

ticle effects consistent with increasing excitation, such as decreasing pairing, lead to an increasing spatial extension of the wave function, as does the use of a finite well. This leads to a decrease of ΔE_c with increasing E_x which is qualitatively consistent with experiment. However, the variations of ΔE_c for low E_x are not reproduced by the calculations. The low values may be occasioned by the $f_{7/2}^{-n}$ character of the low-lying states of $A=51$. Reduction of f-shell Coulomb energies by admixed (sd) holes is noted in Ref. 13.

Although a few clusters of similar resonances suggest some fragmentation of the analog states, too few fragments are identified to justify a detailed analysis, such as that carried out for the $g_{9/2}$ states of $A=51$ (Ref. 1) or the $d_{5/2}$ state of $A=55$.[8]

IV. CONCLUSIONS

The present study completes the systematic γ-spectroscopic survey of the $^{50}Cr+p$ system from 1.0 to 3.36 MeV. In the present work unambiguous spin assignments were made to more than 45 of the 80 resonances detected. Several new analogs were identified, some of which were seen to be fragmented. Altogether in the study, 35 analogs have been proposed, from which the systematic variation of Coulomb energy with excitation energy can be seen. In addition to the $\frac{9}{2}^+$ IAS with its fine structure, two further $\frac{9}{2}^+$ resonances, thought to be core-excited states, were found.

ACKNOWLEDGMENTS

The authors are thankful to the dedicated group of undergraduate students who assisted in the data acquisition. The work was supported by the Research Centre of King Saud University (Project Phys/1406/07) and by the Natural Sciences and Engineering Research Council of Canada.

[1] J. Sziklai, J. A. Cameron, and I. M. Szöghy, Phys. Rev. C **30**, 490 (1984).
[2] G. U. Din, A. M. AlSoraya, J. A. Cameron, V. P. Janzen, and R. B. Schubank, Phys. Rev. C **33**, 103 (1986).
[3] G. U. Din, A. M. AlSoraya, J. A. Cameron, and J. Sziklai, Phys. Rev. C **31**, 1366 (1985).
[4] J. A. Cameron and G. U. Din, Phys. Rev. C **37** (1988).
[5] Zhou Chunmei, Zhou Enchen, Lu Xiane, and Huo Junde, Nucl. Data Sheets **48**, 111 (1986).
[6] J. D. Moses, H. W. Newson, E. G. Bilpuch, and G. E. Mitchell, Nucl. Phys. **A175**, 556 (1971).
[7] T. R. Dittrich, C. R. Gould, G. E. Mitchell, E. G. Bilpuch, and K. Stelzer, Nucl. Phys. **A279**, 430 (1977).
[8] G. U. Din and J. A. Cameron, Phys. Rev. C **35**, 448 (1987).
[9] M. Saltzmann, V. Meyer, and H. Brändle, Nucl. Phys. **A282**, 317 (1977).
[10] E. Arai, M. Futakuchi, J. Komaki, M. Ogawa, and Y. Oguri, J. Phys. Soc. Jpn. **42**, 802 (1983).
[11] W. J. Courtney and J. D. Fox, At. Data Nucl. Data Tables **15**, 141 (1975).
[12] G. U. Din, J. A. Cameron, V. P. Janzen, and R. B. Schubank, Phys. Rev. C **31**, 800 (1985).
[13] J. A. Nolen, Jr. and J. P. Schiffer, Ann. Rev. Nucl. Sci. **19**, 471 (1969).